Development of An Intelligent Marine Engines Health Assessment System Based on Digital-Twins and Data-Driven Models

K. M. Tsitsilonis, Datum Electronics Ltd., konstantinos.tsitsilonis@datum-electronics.co.uk
Prof. G. Theotokatos, Maritime Safety Research Centre, University of Strathclyde, gerasimos.theotokatos@strath.ac.uk
A. Coventry, Datum Electronics Ltd., adrian.coventry@datum-electronics.co.uk

ABSTRACT – ΠΕΡΙΛΗΨΗ

The engine instantaneous torque is a critical measurement which can provide deep insight into the cylinders condition, can be cheaply obtained, and thus also allow for continuous engine monitoring, which is critical in identifying the onset of failures and degradation before incurring increased costs in fuel, spare parts, and vessel down time. This study presents the development of an intelligent engine health assessment system which relies on an engine digital twin, inclusive of both a thermodynamics and a crankshaft dynamics model to simulate the engine's instantaneous torque. Subsequently, the engine digital twin is utilised in tandem with the measured instantaneous torque to successfully identify frequently occurring malfunctioning conditions through an engine faults mapping approach. Furthermore, an even deeper insight to the cylinder's condition is gained, by reconstructing the in-cylinder pressure diagram for all cylinders using just the instantaneous torque.

KEY WORDS - ΛΕΞΕΙΣ ΚΛΕΙΔΙΑ

Instantaneous torque, engine diagnostics, health assessment, torque monitoring, torsional vibration, engine faults mapping.

1. INTRODUCTION – ΕΙΣΑΓΩΓΗ

Shipping is the backbone of global trade and widely recognised as the most energy efficient mode of transportation (Zhang, et al. 2019). Despite this, if shipping was a country, it would be the sixth largest greenhouse gas emitter (Faber, et al. 2020). Hence, as a result of the industry's environmental impact, its global prominence, and the recent movement in public perception, national as well as international organisations and institutions have implemented a series of stringent environmental regulations with ambitious roadmaps such as; the IMO's Data Collection System (DCS) and Energy Efficiency Operational Indicator (EEOI), EU's Monitoring Reporting and Verification (MRV), and UK's Maritime 2050 roadmap to name a few (Monios 2020). This is compelling shipowners to closely monitor and assess the health of their engines to upkeep the ship's operational efficiency to its maximum, which is certainly a non-trivial task considering the complexity of the machinery involved. As a result, this leads to an extensive need of intelligent engine health assessment systems.

Current engine health assessment practices in most cases are primarily reliant on traditional approaches which include manual data entries in logbooks and expert judgement (Hanif Dewan, Omar and Aini 2018). Such manual and empirical approaches are often complemented by one-off inspections, primarily inclusive of lube oil and in-cylinder pressure monitoring, which is critical in providing a deeper insight to the engine's condition. To gain further quantitative insight on the engine's condition, data from the one-off inspections can be analysed in tandem with first-principles models, to diagnose overall engine performance degradation (Kokkulunk, Parlak and Erdem 2016), injectors condition and turbocharger degradation (Hountalas, Kouremenos and M 2004). However,

non-continuous monitoring leaves large time gaps where degradation and failures can develop undetected within the cylinders, amounting to major increases in emissions and fuel consumption, as well as major safety concerns (Malloupas and Yfantis 2021).

Consequently, continuous monitoring is being enabled in a smaller part of the world fleet by the gradual uptake of digitalisation, where peripheral engine measurements are collected such as fuel consumption, cooling water, lube oil and exhaust temperatures at various points before and after the cylinders (Dikis, Lazakis and Turan 2014). However, this acts only as an indirect indicator of the cylinders' health status, and further analysis of these massive data sets requires data-driven models due to their lower computational requirements as compared to first-principles models. In specific, deviations are identified from healthy conditions by incorporating techniques such as Artificial Neural Networks, Bayesian Networks, and clustering algorithms (Gkerekos, Lazakis and Theotokatos 2019, Raptodimos and Lazakis 2018). However, these approaches rely on large sensor networks which demand high capital expenditures, experience data synchronisation issues, and require large training data sets under healthy as well as faulty conditions which can be hard to obtain. This underpins the role of first-principles models, as the means to gain physical understanding and insight to the data obtained from the engine and complement the data-driven models by helping to produce training data sets (Watzenig, Sommer and Steiner 2013).

Alternatively, to continuously obtain insight in the cylinders condition using fewer measurements and minimise sensor installation costs, vibration monitoring is practiced using accelerometers. However, the vibration signals carry substantial noise, which is not related to the combustion process thus greatly complicating the analysis (Bennet, et al. 2017). However, torsional vibration monitoring (or instantaneous torque monitoring) has proven extremely useful by not only identifying mechanical faults in the engine (Lee, et al. 2009), but as shown by recent advances it can potentially reconstruct the in-cylinder pressure diagram for all cylinders using a just a single torque sensor (Tsitsilonis and Theotokatos 2021b). Furthermore, the engine instantaneous torque is a measurement that can be cheaply obtained, the sensors are accurate and reliable, and by extension allows for continuous monitoring of the engine.

In this regard, the aim of this study is to develop an intelligent condition monitoring platform, utilising a combination of instantaneous torque data and engine digital twin models, to perform continuous monitoring and health assessment of the ship's engine, by using a minimal number of sensors.

2. METHODOLOGY

2.1 ENGINE HEALTH ASSESSMENT METHODOLOGY & REFERENCE SYSTEM

The development of an engine health assessment system depends on two critical factors namely; obtain measurements which are both high in accuracy, and carry substantial information regarding the engine's condition, and incorporate a strong algorithm to process said measurements that is able to provide critical information regarding the engine's condition. Thus, the key to the development of this engine health assessment system is the instantaneous torque measurement which is provides critical information, and the two thermodynamics and crankshaft dynamics models which constitute the engine digital twin, that aids in the interpretation of the information provided by the measured data.

In specific, the thermodynamics model takes as input engine constants from the manufacturer manual and the engine shop tests, as well as engine room data including air temperature and cooling water temperatures, as shown in Figure 1. As a result, the engine's thermodynamic performance is replicated accurately across its entire operating envelope at healthy conditions. The output specifically includes the in-cylinder pressure, which is utilised in the crankshaft dynamics model. The crankshaft dynamics

model takes as input engine constants and coefficients from the manufacturer manual, as well as the in-cylinder pressure from the thermodynamics model and returns as output the predicted engine instantaneous torque, for all the engine operating conditions. Subsequently, the combination of the above creates a complete engine digital twin model, which is utilised as a baseline representative of the healthy engine conditions.

Subsequently, as shown in Figure 1, when compared with the instantaneous torque measurements taken in real time, the digital twin can reveal accurately when the engine is experiencing failures and degradation. This is performed by utilising a failure mapping technique presented in (Tsitsilonis and Theotokatos 2021a), where the changes in the instantaneous crankshaft torque measurements with respect to the baseline derived from the digital twin, can be attributed to specific malfunctioning conditions as described further in Section 2.5.

Following the baseline comparison with the failure mapping approach, as shown in Figure 1, a deeper insight can be obtained into the cylinders condition by utilising an inverse crankshaft dynamics model as discussed further below in Section 2.4. In specific, the model utilises the instantaneous torque measured to reconstruct the in-cylinder pressure diagram for all cylinders. This effectively provides the in-cylinder pressures of the engine using a single torque sensor and can do so on a continuous basis to evaluate trends in the changes identified in each in-cylinder pressure diagram.

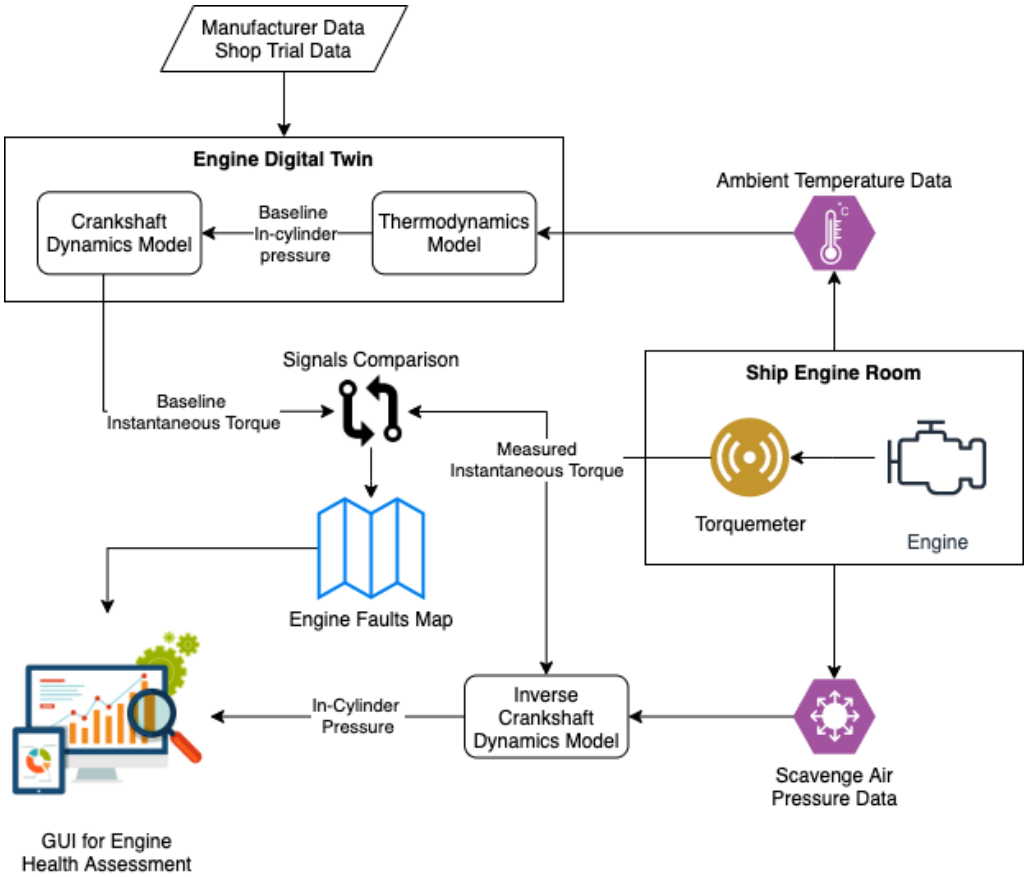

Figure 1: Engine health assessment system schematic.

The usefulness of the above engine health assessment method is presented in Section 3 in the form of a case study, which demonstrates the results of the engine faults map, and the successful implementation of the inverse crankshaft dynamics model, for the case of a reference system. In specific, the reference system utilised for the case study is a 10 cylinder 2-stroke diesel generator with

its basic technical characteristics listed on Table 1. The digital twin for this engine has been developed and validated, in addition to the inverse crankshaft dynamics model. The same methodology can be easily extended to engines utilised in propulsion applications as explained in Section 2.3.

Table 1: Reference system technical characteristics

Number of cylinders	10
Nominal speed	125 rpm
Maximum continuous rating	15.5 MW
Cylinder bore	67 cm

2.2 THERMODYNAMICS MODEL

The thermodynamics model, as shown in its schematic from on Figure 2, was developed to simulate the operation of either a 4-stroke or a 2-stroke engine. In specific, the complete engine including the scavenging ports, exhaust valve and turbocharger were modelled. The engine cylinder processes were modelled using the zero-dimensional approach which employs the mass conservation, energy conservation and ideal gas equation for the calculation of the in-cylinder pressure, temperature, and mixture composition. For the case of the 4-stroke engine, a one zone approach was utilised to model the entire cycle. For the case of the 2-stroke engine, a one-zone approach was utilised to model the closed part of the cycle (compression, combustion, expansion) and the exhaust blow down, whereas a two-zone approach was used to model the scavenging process. The cylinder heat transfer was modelled using the Woschni equation (Woschni 1967), and the Chen-Flynn friction model was employed for calculating the engine friction and mean effective pressure (Pipitone 2009). The combustion model employs the Woschni-Annisits model with a single Wiebe function to calculate the heat release in accordance with the following equation:

$$x_b(\theta) = 1 - \exp\left\{-\alpha\left(\frac{\theta - \theta_{sc}}{\Delta\theta}\right)^{m+1}\right\} \tag{1}$$

where $\alpha = 6.9078$ is the Wiebe function parameter, θ is the crank angle, θ_{sc} is the start of combustion, $\Delta\theta$ is the duration of combustion, and m is the Wiebe exponent. When calculating the start of combustion, the Sitkey equation is considered for the calculation of the injection delay (Merker, et al. 2006).

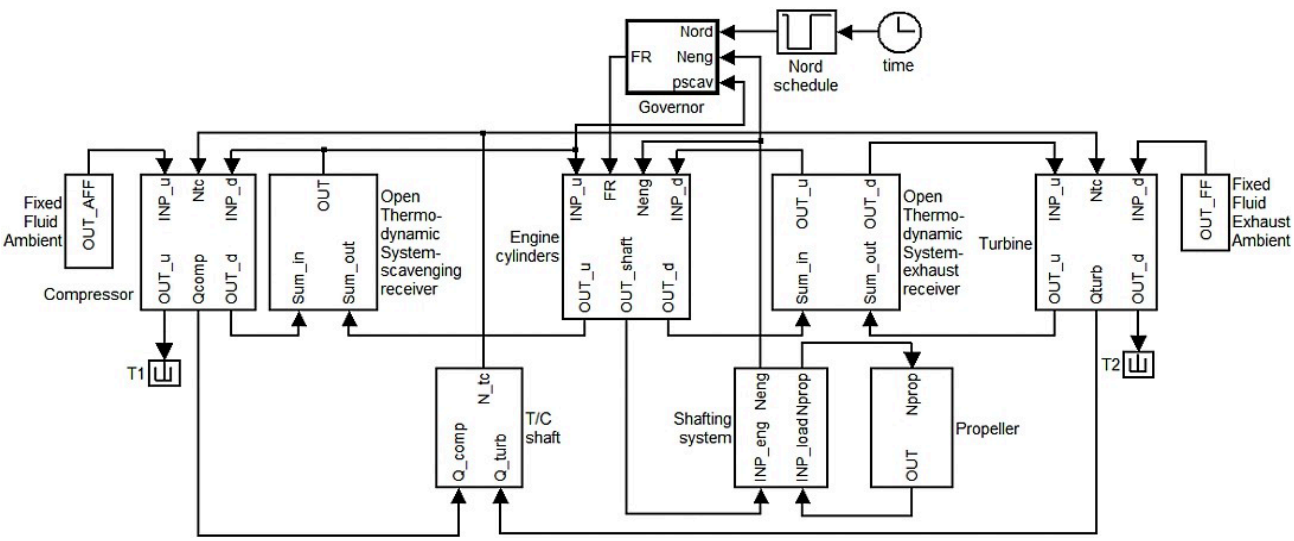

Figure 2: Engine thermodynamics model.

The engine inlet and exhaust manifolds were modelled by using fixed fluid elements, providing the pressure, temperature, and composition of the working media (air or exhaust gas) as input. The model parameters were calibrated to represent the measured data at the engine shop tests with sufficient accuracy. For more details on the model governing equations the reader can refer to (Tsitsilonis and Theotokatos 2021).

2.3 CRANKSHAFT DYNAMICS MODEL

The thermodynamics model was coupled to the crankshaft dynamics model, which is configurable to predict the instantaneous torque for either stationary generators, or propulsion applications. The engine's shaft was modelled by using a lumped mass model, whereby the shaft's mass is concentrated in discrete points referred to as 'inertia disks' along its length, which are connected by stiffness and damping elements as shown in Figure 3 below. This represents the flexibility and structural damping of the shaft, which contributes to the nonlinearities present in the measured instantaneous torque signal. Furthermore, each inertia disk is connected by a damper element to a non-rotating frame of reference, which represents the viscous friction experienced by the engine's bearings. Subsequently, the governing equations of the engine's shafting system are formulated as follows:

$$\boldsymbol{J}\ddot{\boldsymbol{\Theta}} + \boldsymbol{C}\ddot{\boldsymbol{\Theta}} + \boldsymbol{K}\boldsymbol{\Theta} = \boldsymbol{T}_j + \boldsymbol{T}_f + \boldsymbol{T}_c + \boldsymbol{T}_L \tag{2}$$

where $\boldsymbol{J}$, $\boldsymbol{C}$ and $\boldsymbol{K}$ are inertia, damping and stiffness matrices respectively; $\boldsymbol{\Theta}$, $\dot{\boldsymbol{\Theta}}$ and $\ddot{\boldsymbol{\Theta}}$ are vectors of the instantaneous crank angle and its derivatives respectively; and $\boldsymbol{T}_j$, $\boldsymbol{T}_f$, $\boldsymbol{T}_c$, and $\boldsymbol{T}_L$represent the nonlinear inertia torque of the pistons, the engine bearings friction torque, cylinder combustion torque, and the engine load torque. The crankshaft dynamics model can be configured easily for both stationary and propulsion applications, by considering the following equations:

$$T_{L,gen} = k_g \frac{P_{MCR}}{\dot{\theta}_{MCR}} \tag{3}$$

$$T_{L,pro} = k_p \dot{\theta}^n, \text{ where } k_p = \frac{P_{MCR}}{\dot{\theta}_{MCR}^{n+1}} \tag{4}$$

where P_{MCR} and $\dot{\theta}_{MCR}$ are the engine power and speed at the MCR point, k_g with k_p are the generator (Guerrero and Jimenez-Espadafor 2019) and propeller law constants respectively, and $n \approx 2$ is the propeller law exponent (MAN Energy Solutions 2018).

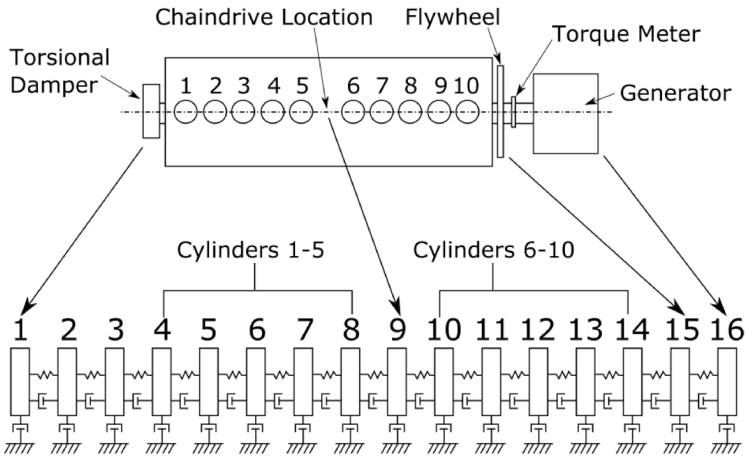

Figure 3: Engine crankshaft dynamics model for a diesel generator.

The variable inertia term is modelled using the constant inertia-speed approach, which greatly simplifies the nonlinearities present in Equation 2 (Schagerberg and McKelvey 2003). Furthermore, the engine bearings friction torque is modelled as being proportional to the instantaneous engine speed, and the engine load is assumed constant in the case of a diesel generator. The crankshaft dynamics model is described in further detail in (K. M. Tsitsilonis, et al. 2020).

2.4 INVERSE CRANKSHAFT DYNAMICS MODEL

The inverse crankshaft dynamics model employs an Initial Value Problem (IVP) technique to reconstruct the in-cylinder pressures using the measured instantaneous torque. In specific, Equation 2 of the crankshaft dynamics problem is repeatedly solved by employing an optimisation algorithm, which varies the parameter values of the in-cylinder pressure curves, such that the simulated instantaneous torque matches the measurements. Therefore, for the case of the 2-stroke reference engine, the in-cylinder pressure curves are parametrised in accordance with the following equation:

$$p_{cy}(\theta) = \{1 - x_b(\theta)\}\, p_{EVC} \left(\frac{V_{EVC}}{V(\theta)}\right)^{\gamma_{co}} + x_b(\theta)\, p_{me} \left(\frac{V_{CL}}{V(\theta)}\right)^{\gamma_{ex}} \tag{5}$$

where p_{EVC} and p_{me} are the pressure at the instant the exhaust valve closes and the maximum isentropic expansion pressure respectively, V_{EVC} and V_{CL} is the volume at the exhaust valve close position and clearance volume respectively, γ_{co} and γ_{ex} are the isentropic compression and expansion coefficients respectively, and $V(\theta)$ is the cylinder volume as a function of crank angle. Subsequently, from Equation 5 the values of p_{EVC}, V_{EVC}, V_{CL}, γ_{co}, γ_{ex} and $V(\theta)$ are all known a-priori using manufacturer and shop trial data. As a result, the IVP technique has to be utilised to estimate the values of the parameters p_{me} from Equation 5, as well as parameters θ_{sc}, $\Delta\theta$, and m which remain unknown from the x_b term, as obtained from Equation 1.

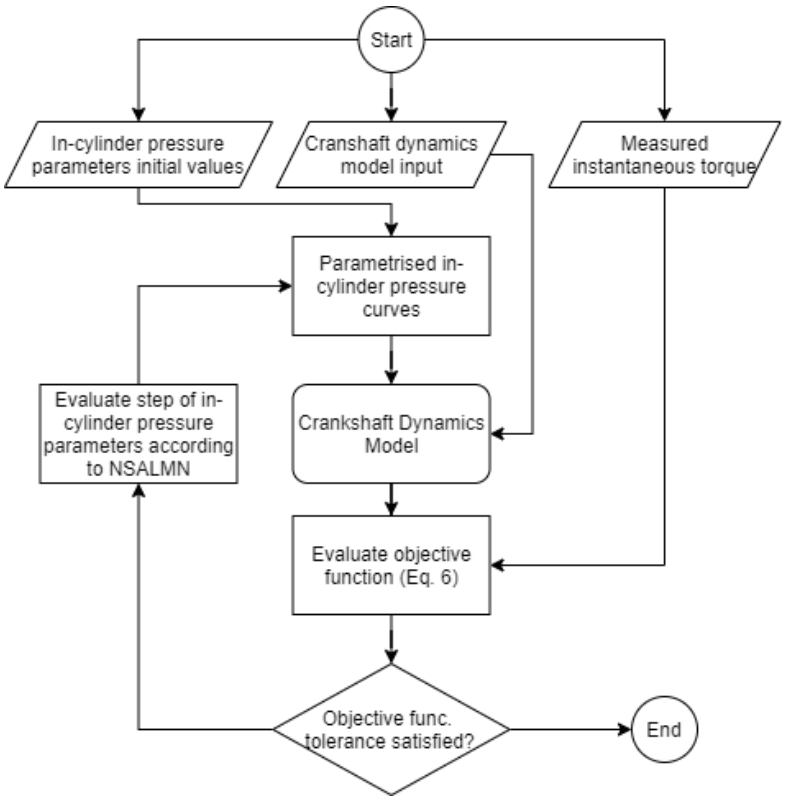

Figure 4: Inverse crankshaft dynamics model algorithm.

Following the parametrisation of the in-cylinder pressure curves, the objective function of the IVP optimisation has to be formulated which is accomplished in accordance with the following equation:

$$O = \frac{1}{2}(T_{sim}([p_{me}, \theta_{sc}, \Delta\theta, m]) - T_{mea})^2 \quad (6)$$

where T_{mea} is the measured instantaneous torque, and T_{sim} is the simulated instantaneous torque, which is a function of the unknown parameters $p_{me}, \theta_{sc}, \Delta\theta, m$. Thus, to solve the IVP Equation 6 has to be minimised, by finding the appropriate values of the aforementioned unknown parameters. To solve this minimisation problem, the Nonmonotone Self-Adaptive Levenberg–Marquardt (NSALMN) algorithm is utilised, which as shown in Figure 4, uses an adaptive iterative approach to solve the aforementioned optimisation problem. For more information regarding the inverse crankshaft dynamics model, refer to (Tsitsilonis and Theotokatos 2021b).

2.5 ENGINE FAULTS MAPPING

To derive the engine faults map, the validated engine digital twin is utilised to simulate four frequently occurring engine malfunctioning conditions, which include: change in the Start of Injection (SOI), change in the Rate of Heat Release (RHR), change in the scavenge air pressure, onset of engine blowby. In specific, for every individual cylinder, 4 model parameters are changed one at a time, to simulate the malfunctioning conditions. A total of 5 simulation runs are performed per parameter to uniformly cover their entire range of values as show in Table 2 below.

Table 2: Malfunctioning conditions parameters variation.

Malfunctioning Condition	Changed Parameter	Parameter Range	Parameter Step
Change in SOI	Start of combustion (θ_{sc})	±2.5º	1.25º
Change in RHR	Wiebe shape parameter (m)	±0.5	0.25
Change in scav. air pressure	Scav. air pressure	±0.3bar	0.15bar
Blowby	Blowby effective area	0~28.5mm^2	7.12 mm^2

Therefore, 5 parametric runs are performed for the first 3 malfunctioning conditions which are; change in SOI change in RHR and blowby, which provides 15 runs per cylinders, giving a total of 150 runs for the 10 cylinders. In addition, the malfunctioning condition of change in scavenge air pressure is implemented to all cylinders simultaneously, which results to an additional 5 runs. By including the healthy engine run, this provides a total of 156 parametric runs of the engine digital twin. From the simulated instantaneous torque signals under malfunctioning conditions, their difference is taken with the healthy engine signal, and a discrete Fourier transform is performed in order to derive the engine faults map. In specific, the faults map identifies which frequency components in the instantaneous torque signal have been affected for each malfunctioning condition introduced to the engine. For further details refer to (Tsitsilonis and Theotokatos 2021a).

3. CASE STUDY

This case study shows the effect of malfunctions on the engine instantaneous torque and the derivation of the faults map, as well as the successful implementation of the inverse crankshaft dynamics model, which demonstrate in principle the benefits and advantages of utilising this engine health assessment system. Firstly, the four frequently occurring malfunctioning conditions as mentioned in Section 2.5 are introduced in the engine digital twin model, and the difference between the healthy engine

instantaneous torque and the torque produced from the malfunctioning conditions is obtained for the sample case of cylinder 2, as shown in Figure 5.

The first malfunctioning conditions examined are the change in SOI and RHR, which indicate engine detuning and/or injectors degradation. It is therefore observed that for the aforementioned malfunctioning conditions, there is a nearly identical change in the engine instantaneous torque. In specific after the malfunctioning cylinder 2 reaches top dead centre, approximately 15 crank angle degrees later, the instantaneous torque difference peaks. This occurs due to the shafting system's flexibility which results to a delay in response from the malfunctioning cylinder firing, and the effect appearing on the flywheel where the torque is measured. Furthermore, the peak in the instantaneous torque performs oscillations which attenuate throughout the entire thermodynamic cycle (360º). For the case of the change in scavenge air pressure, the pattern in the instantaneous torque is noticeably different that the previous malfunctioning conditions. The primary cause is that all cylinders are affected in this case, hence the instantaneous torque does not peak and oscillate, instead a more irregular behaviour is displayed which will be captured by the failure map. Finally, for the case of blowby a similar behaviour in oscillation of the instantaneous torque is displayed after the malfunctioning cylinder reaches top dead centre, however it is noticeably different from all previous cases. The reason primarily lies in the fact that blowby decreases the in-cylinder pressure of the affected cylinder. Therefore, this results to a more regular pattern in the instantaneous torque difference of this malfunctioning condition versus the healthy conditions.

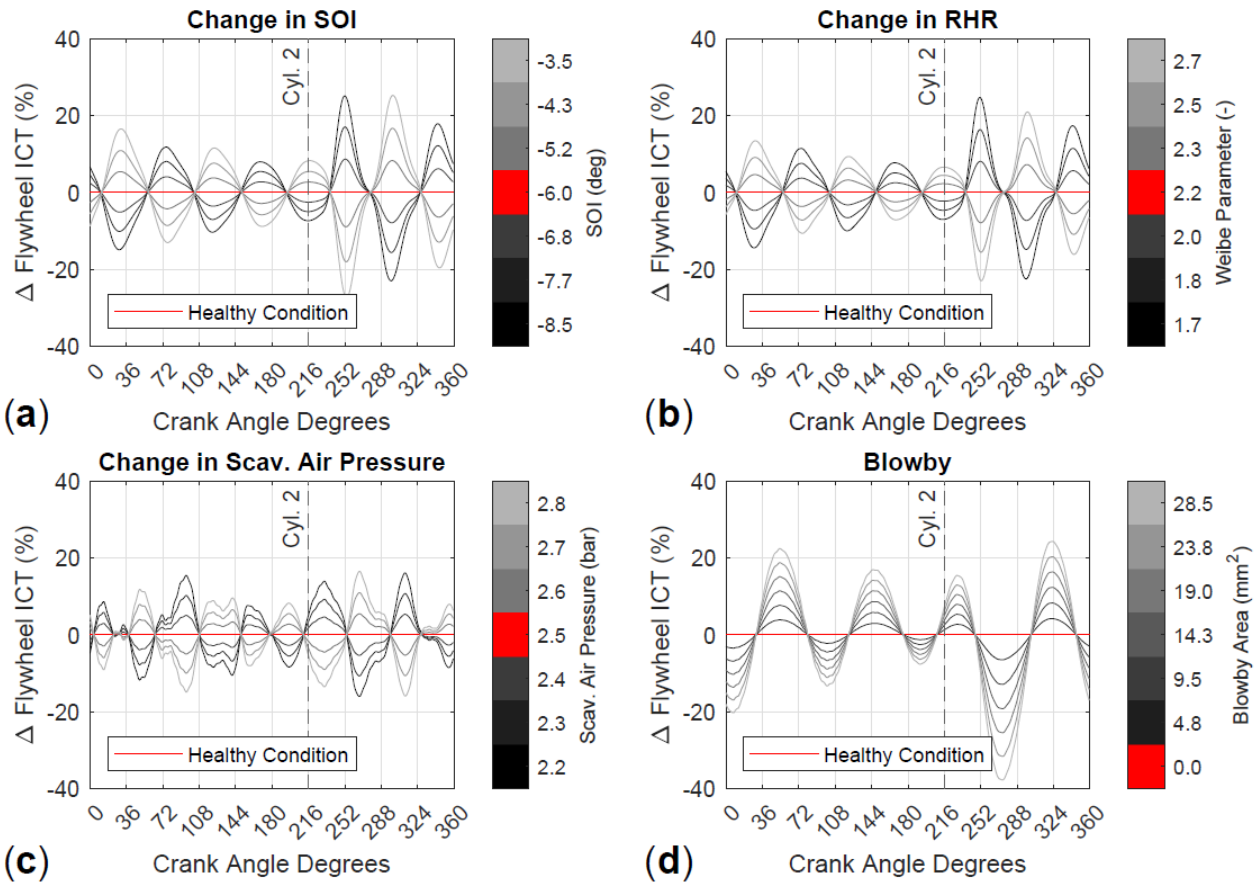

Figure 5: Difference in healthy vs. malfunctioning engine Instantaneous Crankshaft Torque (ICT) measured at the flywheel, for cylinder 2 malfunctioning due to **a)** change in Start of Injection (SOI), **b)** change in Rate of Heat Release (RHR), **c)** change in scavenge air pressure, and **d)** blowby.

Following the above, by performing a discrete Fourier transform of the instantaneous torque signal as described in Section 2.5 above, the engine failure map is constructed as shown in Figure 6. From there, the frequencies of the instantaneous torque effected mostly by the specific malfunctioning conditions can be determined. In specific, it is observed that as described above, the change in SOI and RHR, affect the 4th harmonic frequency for malfunctioning cylinders 3, 5, 6 and 8, as well as the 8th and 9th harmonic frequency for malfunctioning cylinders 4 and 8. Furthermore, distinct harmonic frequencies are affected for the case of blowby as well, where 1st harmonic frequency for malfunctioning cylinders 2-10 and the 4th harmonic frequency for malfunctioning cylinders 1, 2, 3 and 10 is affected. Similarly for the change in scavenge air pressure the 3rd and 5th harmonic frequencies are affected distinctly for all engine cylinders malfunctioning. As a result, the above suffices to diagnose blowby or a change in scavenge air pressure if they occur individually to any of the engine's 10 cylinders respectively.

Hence by simply conducting a frequency analysis on the measured torque signal, its frequency components can be compared to the baseline derived from the digital twin and referenced against the engine faults map, which will be able to identify any malfunctioning conditions such as the ones mentioned in this study.

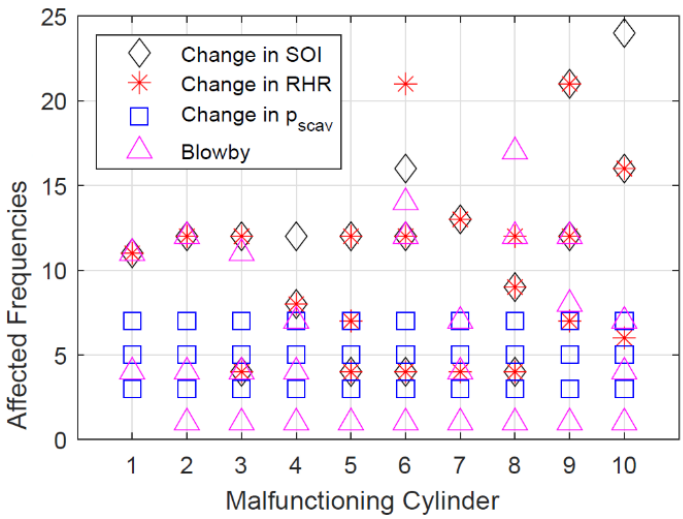

Figure 6: Engine faults map

Having gained insight into the cylinders condition using the mapping technique above, the inverse crankshaft dynamics model can be utilised to gain even deeper insight into the cylinders condition by reconstructing the in-cylinder pressure for all of the engine's cylinders using the measured instantaneous crankshaft torque. The capability of the inverse model is going to be demonstrated in its prediction of the in-cylinder pressure diagrams of a heavily degraded engine, as shown in Figure 7.

In specific, the engine digital twin of the reference was used to simulate both the in-cylinder pressure and the instantaneous torque of a heavily degraded engine. This was accomplished by setting a random number generator to generate values which lie within their respective parameter range for the four malfunctioning conditions listed on Table 2. Subsequently, by utilising the instantaneous torque for the heavily degraded engine shown as measured torque in Figure 7, the inverse crankshaft dynamics model was used. It is therefore visible from Figure 7 that the inverse crankshaft dynamics model was able to successfully predict the in-cylinder pressure diagram, even when large variations between the engine malfunctioning condition parameters were present. The error in the pressure prediction was

three orders of magnitude less than the peak in-cylinder pressure, so that demonstrates adequate performance.

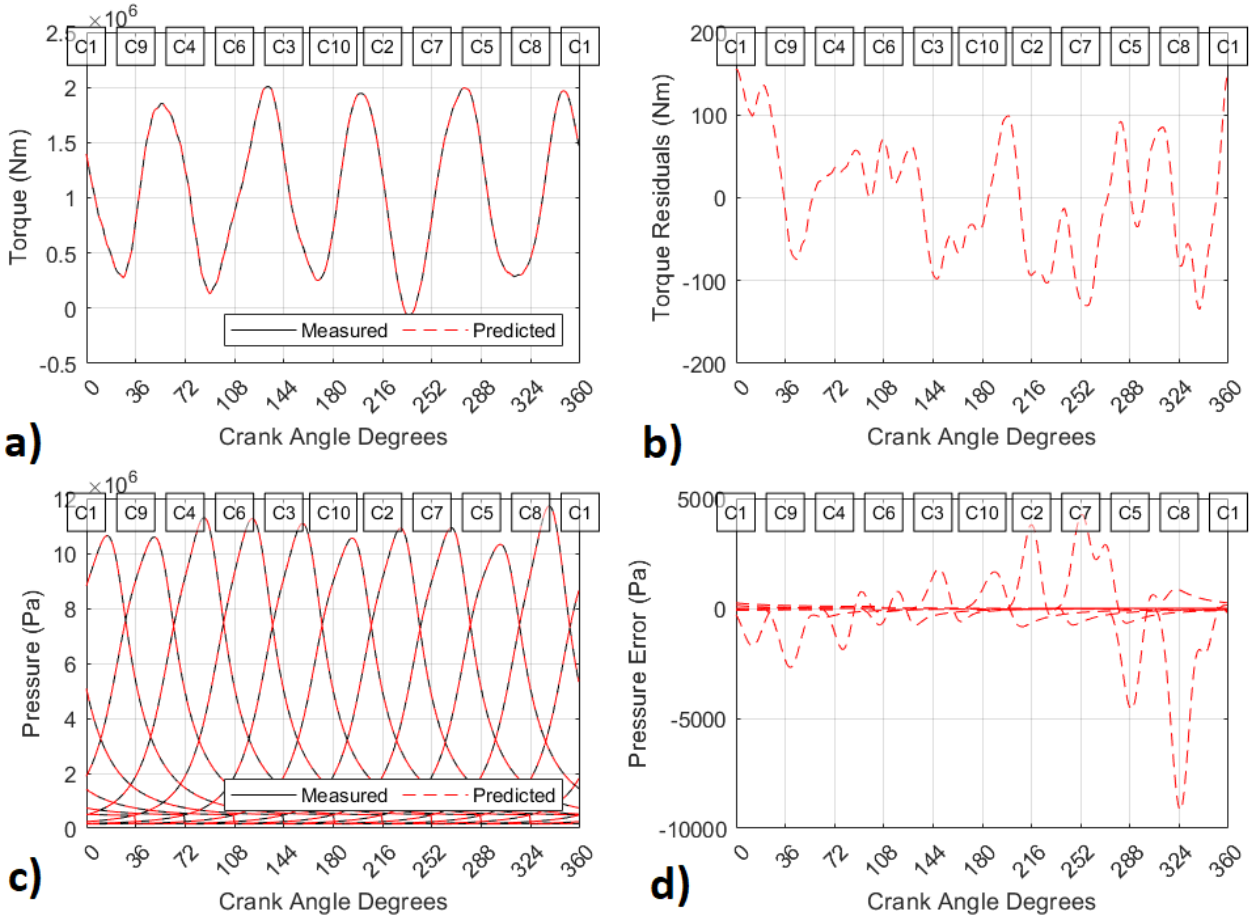

Figure 7: Inverse crankshaft dynamics model in-cylinder pressure prediction on heavily degraded engine.

The inverse crankshaft dynamics model represents a novel method of utilising engine models to place virtual sensors within the engine. Hence, by considering a non-intrusive and cheap measurement such as the instantaneous torque, multiple other critical measurements from the engine can be predicted such as the in-cylinder pressures in this case, which greatly reduces the costs and expands engine insight and diagnostic capabilities.

7. CONCLUSION – ΣΥΜΠΕΡΑΣΜΑΤΑ

This study presents an intelligent engine health assessment system which utilises the engine instantaneous torque measurements to perform critical diagnostics functions. The engine instantaneous torque is a reliable and cheap measurement to obtain, that can provide critical information regarding the engine's health status. Therefore, by utilising state-of-the-art engine digital twins and health assessment algorithms, it was demonstrated that the instantaneous crankshaft torque can be employed to determine frequently occurring malfunctioning conditions including change in Start of Injection (SOI), change in Rate of Heat Release (RHR), change in scavenge air pressure, and blowby. Specifically, it was proven that when cylinders individually undergo these malfunctions, distinct frequency components of the instantaneous torque are affected, which when mapped, can be compared to the engine's actual operation to diagnose such malfunctions. Furthermore, to gain an even deeper level of insight to the cylinder's condition, an inverse crankshaft dynamics model was

utilised which successfully predicted the in-cylinder pressure for all cylinders, using the measured instantaneous torque. As a result, this demonstrates the usefulness of this measurement, particularly when employed in tandem with engine digital twins.

Future work will include validation of the digital twins and inverse crankshaft dynamics model in 4-stroke engines as well. Further expansion of this engine health assessment system can be made, utilising digital twins with enhanced capabilities to provide information on engine emissions as well.

8. ACKNOWLEDGEMENTS – ΕΥΧΑΡΙΣΤΙΕΣ

The authors from MSRC greatly acknowledge the funding from DNV AS and RCCL for the MSRC establishment and operation. Additionally, the authors gratefully acknowledge the financial support of Innovate UK, through the Knowledge Transfer Partnership project (project number 11577), for the work reported in this paper. The opinions expressed herein are those of the authors and should not be construed to reflect the views of Innovate UK, DNV AS and RCCL.

9. BIBLIOGRAPHY – ΒΙΒΛΙΟΓΡΑΦΙΑ

Bennet, Colin, J.F. Dunne, S. Trimby, and Richardson D. 2017. "Engine cylinder pressure reconstruction using crank kinematics and recurrently-trained neural networks." *Mechanical Systems and Signal Processing* 85: 126-145.

Dikis, Konstantinos, Iraklis Lazakis, and Osman Turan. 2014. "Probabilistic Risk Assessment of Condition Monitoring of Marine Diesel Engines." Glasgow: International Conference on Maritime Technology.

Faber, Jasper, Shinichi Hanayama, Shuang Zhang, Paula Pereda, Bryan Comer, Elena Hauerhof, Wendela Schim van der Loeff, et al. 2020. *Fourth IMO GHG Study 2020.* London: International Maritime Organisation.

Gkerekos, Christos, Iraklis Lazakis, and Gerasimos Theotokatos. 2019. "Machine learning models for predicting ship main engine Fuel Oil Consumption: A comparative study." *Ocean Engineering* 188 (106282).

Guerrero, Daniel Palomo, and Francisco J. Jimenez-Espadafor. 2019. "Torsional system dynamics of low speed diesel engines based on instantaneous torque: Application to engine diagnosis." *Mechanical Systems and Signal Processing* 116: 858-878. doi:https://doi.org/10.1016/j.ymssp.2018.06.051.

Hanif Dewan, Mohammud, Yaakob Omar, and Suzana Aini. 2018. "Barriers for adoption of energy efficiency operational measures in shipping industry ." *WMU Journal of Maritime Affairs* 17: 169-193.

Hountalas, DT, DA Kouremenos, and Sideris M. 2004. "A Diagnostic Method for Heavy-Duty Diesel Engines Used in Stationary Applications." *Journal of Engineering for Gas Turbines and Power* 126 (4): 886-898.

Kokkulunk, Gorkem, Andan Parlak, and Hasan Huseyin Erdem. 2016. "Determination of performance degradation of a Marine Diesel Engine by using curve based approach." *Applied Thermodynamics* 108: 1136-1146.

Lee, D.C., K.S. Joo, T.K. Nam, E.S. Kim, and Kim S.H. 2009. "Development of engine vibration analysis and monitoring system (EVAMOS) for marine vessels." *Transactions of the Korean society for noise and vibration engineering* 19 (2): 155-161.

Malloupas, George, and Elias Ar. Yfantis. 2021. "Decarbonization in Shipping Industry: A Review of Research, Technology Development, and Innovation Proposals." *Journal of Marine Science and Engineering* 415 (9).

MAN Energy Solutions. 2018. "man-es.com." 10. Accessed 08 10, 2021. https://man-es.com/docs/default-source/marine/5510-0004-04_18-1021-basic-principles-of-ship-propulsion_web.pdf?sfvrsn=5083eaa8_4.

Merker, Gunter P., Christian Schwarz, Gunnar Stiesch, and Frank Otto. 2006. *Simulation Combustion - Simulation of combustion and pollutant formation for engine-development.* Berlin: Springer-Verlag.

Monios, Jason. 2020. "Environmental governance in shipping and ports: Sustainability and scale challenges." In *Maritime Transport and Regional Sustainability*, edited by Adolf K.Y. Ng, Jason Monios and Changmin Jiang, 13-29. Amsterdam: Elsevier.

Pipitone, Emiliano. 2009. "A New Simple Friction Model for S.I. Engine." *SAE International.*

Raptodimos, Yannis, and Iraklis Lazakis. 2018. "Using artificial neural network-self-organising map for data clustering of marine engine condition monitoring applications." *Ships and Offshore Structures* 13 (6): 649-656.

Schagerberg, Stefan, and Tomas McKelvey. 2003. "Instantaneous Crankshaft Torque Measurements - Modeling and Validation." *SAE International.*

Tsitsilonis, Konstantinos M, Gerasimos Theotokatos, Nikolaos Xiros, and Malcolm Habens. 2020. "Systematic investigation of a large two-stroke engine crankshaft dynamics model." *Energies* 2486 (13). doi:doi:10.3390/en13102486.

Tsitsilonis, Konstantinos M., and Gerasimos Theotokatos. 2021a. "Engine malfunctioning conditions identification through instantanous crankshaft torque measurement analysis." *Applied Sciences* 11.

Tsitsilonis, Konstantinos Marios, and Gerasimos Theotokatos. 2021b. "A novel method for in-cylinder pressure prediction using the engine instantaneous crankshaft torque." *Journal of Engineering for the Maritime Environment* M: 1-19.

Watzenig, Daniel, Martin S. Sommer, and Gerald Steiner. 2013. "Model-Based Condition and State Monitoring of Large Marine Diesel Engines." In *Diesel Engine - Combustion, Emissions and Condition Monitoring*, edited by Saiful Bari, 217-230. London: IntechOpen.

Woschni, Gerhard. 1967. "A universally applicable equation for the instantanesous heat transfer coefficient in the internal combustion engine." *SAE International* (SAE).

Zhang, Shuang, Ying Li, Haichao Yuan, and Deping Sun. 2019. "An alternative benchmarking tool for operational energy efficiency of ships and its policy implications." *Journal of Cleaner Production* 240: 118-223.